

## Determination of $\Gamma_{ee}$ of the $\Upsilon(1S)$ and $\Upsilon(2S)$ resonances, and measurement of $R$ at $W = 9.39$ GeV

Crystal Ball Collaboration

Z. Jakubowski<sup>3</sup>, D. Antreasyan<sup>8</sup>, H.W. Bartels<sup>4</sup>, D. Besset<sup>10</sup>, Ch. Bieler<sup>7</sup>, J.K. Bienlein<sup>4</sup>, A. Bizzeti<sup>6</sup>, E.D. Bloom<sup>11</sup>, I. Brock<sup>2</sup>, K. Brockmüller<sup>4</sup>, R. Cabenda<sup>10</sup>, A. Cartacci<sup>6</sup>, M. Cavalli-Sforza<sup>a,10</sup>, R. Clare<sup>11</sup>, A. Compagnucci<sup>6</sup>, G. Conforto<sup>6</sup>, R. Cowan<sup>10</sup>, D. Coyne<sup>a,10</sup>, G. Drews<sup>4</sup>, A. Engler<sup>2</sup>, K. Fairfield<sup>11</sup>, G. Folger<sup>5</sup>, A. Fridman<sup>c,11</sup>, J. Gaiser<sup>11</sup>, D. Gelphman<sup>11</sup>, G. Glaser<sup>5</sup>, G. Godfrey<sup>11</sup>, K. Graaf<sup>7</sup>, F.H. Heimlich<sup>7</sup>, F.H. Heinsius<sup>7</sup>, R. Hofstadter<sup>11</sup>, J. Irion<sup>8</sup>, H. Janssen<sup>9</sup>, K. Karch<sup>12</sup>, S. Keh<sup>12</sup>, T. Kiel<sup>7</sup>, H. Kilian<sup>12</sup>, I. Kirkbride<sup>11</sup>, T. Kloiber<sup>4</sup>, M. Kobel<sup>5</sup>, W. Koch<sup>4</sup>, A.C. König<sup>9</sup>, K. Königsmann<sup>12</sup>, R.W. Kraemer<sup>2</sup>, S. Krüger<sup>7</sup>, G. Landi<sup>6</sup>, R. Lee<sup>11</sup>, S. Leffler<sup>11</sup>, R. Lekebusch<sup>7</sup>, A.M. Litke<sup>11</sup>, W. Lockmann<sup>11</sup>, S. Lowe<sup>11</sup>, B. Lurz<sup>5</sup>, D. Marlow<sup>2</sup>, H. Marsiske<sup>4</sup>, W. Maschmann<sup>7</sup>, P. McBride<sup>8</sup>, H. Meyer<sup>4</sup>, B. Muryn<sup>3</sup>, F. Messing<sup>2</sup>, W.J. Metzger<sup>9</sup>, B. Monteleoni<sup>6</sup>, R. Nernst<sup>7</sup>, B. Niczyporuk<sup>11</sup>, G. Nowak<sup>3</sup>, C. Peck<sup>1</sup>, C. Pegel<sup>7</sup>, P.G. Pelfer<sup>6</sup>, B. Pollock<sup>11</sup>, C. Pols<sup>9</sup>, F.C. Porter<sup>1</sup>, D. Prindle<sup>2</sup>, P. Ratoff<sup>1</sup>, M. Reidenbach<sup>9</sup>, B. Renger<sup>2</sup>, C. Rippich<sup>2</sup>, M. Scheer<sup>12</sup>, P. Schmitt<sup>12</sup>, J. Schotanus<sup>9</sup>, J. Schütte<sup>5</sup>, A. Schwarz<sup>11</sup>, F. Selonke<sup>4</sup>, D. Sievers<sup>7</sup>, T. Skwarnicki<sup>4</sup>, V. Stock<sup>7</sup>, K. Strauch<sup>8</sup>, U. Strohmusch<sup>7</sup>, J. Tompkins<sup>11</sup>, H.J. Trost<sup>4</sup>, B. van Uiter<sup>11</sup>, R.T. Van de Walle<sup>9</sup>, H. Vogel<sup>2</sup>, A. Voigt<sup>4</sup>, U. Volland<sup>5</sup>, K. Wachs<sup>4</sup>, K. Wacker<sup>11</sup>, W. Walk<sup>9</sup>, H. Wegener<sup>5</sup>, D. Williams<sup>8</sup>, P. Zschorsch<sup>4</sup>

<sup>1</sup> California Institute of Technology, Pasadena, CA 91125, USA

<sup>2</sup> Carnegie-Mellon University, Pittsburgh, PA 15213, USA

<sup>3</sup> Cracow Institute of Nuclear Physics, PL-30055 Cracow, Poland

<sup>4</sup> Deutsches Elektronen Synchrotron DESY, D-2000 Hamburg, Federal Republic of Germany

<sup>5</sup> Universität Erlangen-Nürnberg, D-8520 Erlangen, Federal Republic of Germany

<sup>6</sup> INFN and University of Firenze, I-50100 Firenze, Italy

<sup>7</sup> Universität Hamburg, I. Institut für Experimentalphysik, D-2000 Hamburg, Federal Republik of Germany

<sup>8</sup> Harvard University, Cambridge, MA 02138, USA

<sup>9</sup> University of Nijmegen and NIKHEF NL-6525 ED Nijmegen, The Netherlands

<sup>10</sup> Princeton University, Princeton, NJ 08544, USA

<sup>11</sup> Department of Physics, HEPL, and Stanford Linear Accelerator Center, Stanford University, Stanford, CA 94305, USA

<sup>12</sup> Universität Würzburg, D-8700 Würzburg, Federal Republic of Germany

Received 24 March 1988

**Abstract.** Using the Crystal Ball detector operating at the DORIS II storage ring we have measured the leptonic partial widths  $\Gamma_{ee}$  of the  $\Upsilon(1S)$  and  $\Upsilon(2S)$  resonances. We find

$$\Gamma_{ee}(\Upsilon(1S)) = 1.34 \pm 0.03 \pm 0.06 \text{ keV}$$

and

$$\Gamma_{ee}(\Upsilon(2S)) = 0.56 \pm 0.04 \pm 0.02 \text{ keV.}$$

The effect on  $\Gamma_{ee}$  of applying different prescriptions for radiative corrections is discussed. We also measure  $R$ , the ratio of non-resonant hadronic cross section to the Born cross section of  $\mu$  pair production, at c.m. energy  $W = 9.39$  GeV to be

$$R = 3.48 \pm 0.04 \pm 0.16.$$

<sup>a</sup> Present Address: Inst. for Particle Physics, University of California, Santa Cruz, CA 95064, USA

<sup>b</sup> Present Address: Massachusetts Institute of Technology, Cambridge, MA 02139, USA

<sup>c</sup> Permanent Address: DPHPE, Centre d'Etudes Nucléaires de Saclay, F-91191 Gif sur Yvette, France

## 1 Introduction

Ever since the discovery [1] of the  $Y$  resonances in 1977 measurements of their leptonic partial decay widths  $\Gamma_{ee}$  have been of great interest. The measured values support the interpretation of the  $Y$  family as bound states of charge  $|q|=1/3$  particles and serve as tests for potential models, which describe the  $Y(nS)$  as the  $n^3S_1$  states of a  $b\bar{b}$  system. Moreover, the total widths  $\Gamma_{\text{tot}}$  are usually obtained from the measured  $\Gamma_{ee}$  widths via the relation  $\Gamma_{\text{tot}}=\Gamma_{ee}/B_{\mu\mu}$ , where  $B_{\mu\mu}$  is the independently measured  $Y(nS)$  decay branching ratio to  $\mu$  pairs. This assumes lepton universality, which will be done throughout this paper.

We report here a precision measurement of  $\Gamma_{ee}$  for the  $Y(1S)$  and  $Y(2S)$  resonances performed with the Crystal Ball detector operating at the DORIS II  $e^+e^-$  storage ring at DESY.  $\Gamma_{ee}$  is obtained from the measurement of the cross section for  $e^+e^- \rightarrow \text{hadrons}$  as a function of the  $e^+e^-$  center-of-mass (c.m.) energy  $W$  in the region of the resonance. We use 4 scans of the  $Y(1S)$  and one of the  $Y(2S)$ . From continuum data taken below the  $Y(1S)$  and from the  $Y(1S)$  scans we also obtain a value of  $R$ , the ratio of non-resonant hadronic cross section to the Born cross section of  $\mu$  pair production, at  $W=9.39$  GeV. Single beam data is used in the background estimates.

Extracting  $\Gamma_{\text{tot}}$  from  $\Gamma_{ee}/B_{\mu\mu}$  requires consistent application of radiative corrections in the separate determinations of  $\Gamma_{ee}$  and  $B_{\mu\mu}$ , which has not been the case for previously quoted values of  $\Gamma_{\text{tot}}$  for the  $Y$  resonances. We use consistent definitions of  $\Gamma_{ee}$  and  $B_{\mu\mu}$  which correspond to the  $Y$  decay to *all*  $e^+e^-$  and  $\mu^+\mu^-$  final states: the contributions of higher order QED diagrams to the *decays* are *not* removed. We compare our result to previous  $\Gamma_{ee}$  measurements by re-normalizing these to correspond to the radiative corrections as applied here. In obtaining the value of  $R$  we follow its traditional definition: the ratio of the QED lowest order continuum cross sections for  $e^+e^- \rightarrow \text{hadrons}$  and  $e^+e^- \rightarrow \mu^+\mu^-$ .

This paper is organized as follows: Section 2 gives a short description of the Crystal Ball detector. The hadronic event selection criteria are discussed in Sect. 3. The Monte Carlo event generation used in determining efficiencies to observe hadronic events is described in Sect. 4. Section 5 is devoted to the backgrounds in the hadronic data sample. The luminosity determination is discussed in Sect. 6. Since  $\Gamma_{ee}$  and in turn  $\Gamma_{\text{tot}}$  depend strongly on the parametrization used for the observed cross section  $\sigma^{\text{obs}}(W)$ , we discuss the different theoretical formulations for it in some detail in Sect. 7. In Sect. 8 we describe our procedure to determine  $\Gamma_{ee}$  and present our results. The effect on  $\Gamma_{ee}$  of different theoretical formulations for  $\sigma^{\text{obs}}(W)$

is discussed in Sect. 9. The measurement of  $R$  is described in Sect. 10, which is followed by our conclusions.

## 2 Detector and trigger

The Crystal Ball detector [2] is a non-magnetic calorimeter designed to measure precisely the energies and directions of electromagnetically interacting particles. The experimental setup is shown in Fig. 1. The main detector is a spherical shell of 672 optically isolated NaI(Tl) crystals covering 93% of the total solid angle. The remaining 7% is left free to allow room for the beam pipe. Each crystal, of truncated pyramidal shape, is 16 radiation lengths deep (corresponding to  $\sim 1$  nuclear absorption length), points to the interaction region and is read out by its own photomultiplier. The 60 crystals immediately surrounding the beam pipe are called ‘‘tunnel crystals’’. They cover the angular region of approximately  $0.85 < |\cos \theta| < 0.93$ , where  $\theta$  is the angle with respect to the beam axis. NaI(Tl) endcaps increase the angular coverage to 98% of  $4\pi$ , but are not used in this analysis.

The measured energy resolution for electromagnetically showering particles is  $\sigma_E/E = (2.7 \pm 0.2)\% \sqrt[4]{E/\text{GeV}}$ . Minimum ionizing particles deposit about 210 MeV. Approximately two thirds of the hadrons are expected to undergo nuclear interactions while traversing the NaI(Tl). The directions of electromagnetically showering particles are measured in the NaI(Tl) to an accuracy of  $\sigma_\theta = 1^\circ$  to  $2^\circ$ , depending on their energy. For minimum ionizing particles  $\sigma_\theta \approx 3^\circ$ .

The data used in this analysis satisfy our total energy trigger, which is fully efficient for events depositing at least 1.9 GeV in the NaI(Tl) crystals which lie within  $|\cos \theta| < 0.85$ . Our selected hadronic events (see Sect. 3) have a minimum total energy of  $\sim 2.1$  GeV.

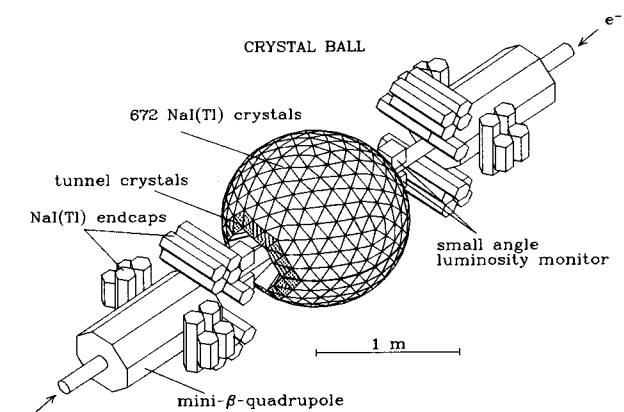


Fig. 1. View of the Crystal Ball detector

### 3 Hadronic event selection

The criteria to select hadronic events are designed to have a high detection efficiency while reducing background contributions to a minimum, thus minimizing systematic effects. We rely solely on the most accurate and efficient part of the detector: the 672 NaI(Tl) crystals of the main ball. We define the energy seen in the 672 crystals as  $E_{\text{BALL}} = \sum_{i=1}^{672} E_i$  and

an energy cluster as a group of adjacent crystals with energies greater than 10 MeV each. Hadronic events then have to pass the following selections cuts:

1.  $0.2W \leq E_{\text{BALL}} \leq 1.1W$ , where  $W$  is the c.m. energy.
2.  $E_{\text{tunnels}}/E_{\text{BALL}} < 0.5$ , where  $E_{\text{tunnels}}$  is the sum of the energies deposited in the 60 tunnel crystals of the main ball.

3. As a measure of the energy imbalance of an event we define  $\beta \equiv |\beta| = \frac{1}{E_{\text{BALL}}} \left| \sum_{i=1}^{672} E_i \hat{n}_i \right|$ , where  $\hat{n}_i$  is a unit

vector pointing to the center of the  $i^{\text{th}}$  crystal. The normalized transverse energy of an event is defined

as  $x_{\text{tr}} = \frac{1}{W} \sum_{i=1}^{672} E_i \sin \theta_i$ . Guided by Monte Carlo studies of hadronic events we apply the following cuts

in the  $(\beta, x_{\text{tr}})$  plane: events are accepted if they satisfy  $x_{\text{tr}} > 0.23$ ,  $\beta < 0.7$  and  $x_{\text{tr}} > 0.5\beta + 0.11$ . These cuts are shown in Fig. 2, where we present in the  $(\beta, x_{\text{tr}})$  plane the event population for a representative subsample of unselected data.

4. There should be at least 3 energy clusters with an energy  $E_{\text{cluster}} > 100$  MeV each.
5. Events should not have more than 1 energy cluster with  $E_{\text{cluster}} > 0.35W$ .

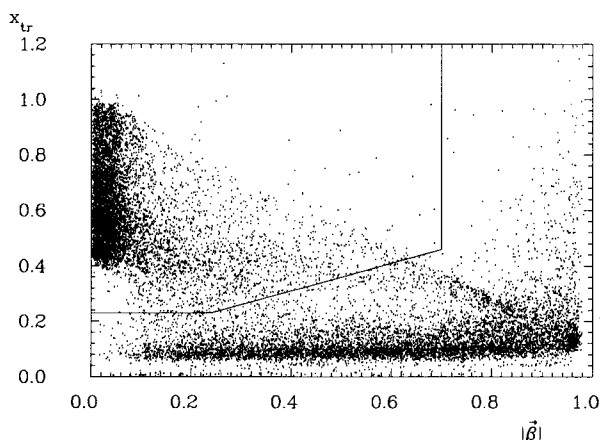


**Fig. 2.**  $(\beta, x_{\text{tr}})$  plane for unselected data. The accepted events are in the upper left corner separated from the rejected events by the solid line (see text)

6. Events should not have any energy cluster with  $E_{\text{cluster}} > 0.35W$  if  $E_{\text{BALL}} > 0.75W$ .

Cuts 1 to 4 are effective in suppressing backgrounds coming from beam-gas interactions, cosmics and two-photon collisions. The last two cuts efficiently remove background from QED processes like Bhabha scattering. The background remaining in our hadronic data sample is discussed in detail in Sect. 5.

### 4 Efficiency determination

The detection efficiencies for hadronic events from  $Y(1S)$  and  $Y(2S)$  decays, continuum  $q\bar{q}$  production events and background events are calculated using the Monte Carlo technique. Hadronic events from  $Y(1S)$  and  $Y(2S)$  decays and from continuum  $q\bar{q}$  production are generated with the standard LUND string fragmentation program version 6.2 [3]. As an alternative hadronization scheme we use the coherent parton shower model offered in the same program. This scheme is based on the QCD cascade model by Marchesini and Webber [4]. In Sects. 8 and 10 we estimate our sensitivity to the hadronization scheme from the difference in the efficiencies obtained with the two models.

The generated events are passed through a complete detector simulation. This simulation includes the following steps:

1. Electromagnetically interacting particles are handled by the electromagnetic shower development program EGS [5].
2. The interactions of hadrons are simulated with the GHEISHA 6 program [6].
3. Extra energy deposited in the crystals by beam-related background is taken into account by adding special background events to the Monte Carlo events. These background events are obtained by triggering on every  $10^7$ th beam crossing, with no other condition.
4. The events are then reconstructed using our standard software and subjected to the same cuts as the data.

The efficiency calculations are described in more detail in Sects. 5, 8 and 10.

### 5 Backgrounds

Background events originate from 1) QED processes, 2) two-photon interactions and 3) collisions of beam particles with residual gas and the vacuum beam pipe. Estimates of the magnitudes of these backgrounds are obtained with Monte Carlo techniques and single beam data. The specific method used depends on the origin of the background events and will be discussed

below. The resulting background estimates will be used in Sects. 8 and 10 in the determination of  $\Gamma_{ee}$  and  $R$ , respectively, and in the estimate of the systematic errors.

### 5.1 QED processes

To estimate the background from the QED processes  $e^+e^- \rightarrow e^+e^-(\gamma)$ ,  $\gamma\gamma(\gamma)$ ,  $\mu^+\mu^-(\gamma)$ , and  $e^+e^- \rightarrow \tau^+\tau^-(\gamma)$ , we generate events of these types with the programs of Berends et al. [7, 8]. The  $(\gamma)$  indicates that photon emission and other QED processes to  $\mathcal{O}(\alpha^3)$  are included. The generated cross sections  $\sigma$  and their products with the corresponding efficiencies  $\varepsilon$  to pass our hadronic selection cuts are presented in Table 1. The largest source of background stems from the  $e^+e^- \rightarrow \tau^+\tau^-(\gamma)$  channel with  $\varepsilon\sigma = 171 \pm 4$  pb compared to  $\varepsilon\sigma \approx 3000$  pb for  $e^+e^- \rightarrow \text{hadrons}$  at  $W = 9.39$  GeV. Contributions from the other QED reactions are much smaller.

### 5.2 Two-photon collisions

According to a recent compilation [9] of the total cross section data of the process  $\gamma\gamma \rightarrow \text{hadrons}$  a good description of this data is obtained by adding the predictions of the generalized vector-meson dominance model (GVDM) and the quark parton model (QPM). Since we expect only small background contributions from two-photon interactions we follow this suggestion. For the QPM part we generate  $q\bar{q}$  pairs with a Monte Carlo program of Vermaseren and Lepage [10] with subsequent hadronization by the standard LUND program version 6.2 [3]. Two-photon events with a GVDM cross section, parametrized according to [9] as  $\sigma_{\text{tot}}(\gamma\gamma \rightarrow \text{hadrons}) = [(240 \pm 29) + (394 \pm 110) \text{ GeV}/W_{\gamma\gamma}]$  nb, are generated by a Monte Carlo program using the equivalent photon approximation [11]. The sum of the generated QPM and GVDM cross sections and the resulting observable cross section are presented in Table 1.

### 5.3 Beam-gas background

Events from collisions of beam particles with residual gas or with the vacuum pipe are referred to as ‘‘beam-

**Table 1.** Summary of Monte Carlo generated continuum QED and two-photon cross sections  $\sigma$  and observed cross sections  $\varepsilon\sigma$ . The errors in  $\varepsilon\sigma$  originate from Monte Carlo statistics

Process	$W[\text{GeV}]$	$\sigma[\text{nb}]$	$\varepsilon\sigma[\text{pb}]$
$e^+e^- \rightarrow e^+e^-(\gamma)$	9.39	103.9	$14.6 \pm 4.1$
$e^+e^- \rightarrow \gamma\gamma(\gamma)$	9.39	31.3	$1.3 \pm 0.3$
$e^+e^- \rightarrow \mu^+\mu^-(\gamma)$	9.39	1.4	$< 1$
$e^+e^- \rightarrow \tau^+\tau^-(\gamma)$	9.39	1.1	$171 \pm 4$
$\gamma\gamma \rightarrow \text{hadrons}$	9.39	7.1	$19.8 \pm 5.6$

gas’’ events. The contamination from beam-gas events in our hadronic sample is determined from single  $e^+$  and  $e^-$  beam runs taken close in time to our resonance scans. We assume that all events in the single beam data which meet our selection criteria are beam-gas events. The number of residual beam-gas events in the hadron selected colliding beam data sample is calculated in two independent ways.

In the first method we normalize the single beam data to the colliding beam data by integrating the product of the total beam current and the gas pressure over run time. This method is essentially independent of any model, but sensitive to any difference in beam optics between single beam and colliding beam runs.

The second method makes use of Monte Carlo simulations. For a given set of hadronic event selection criteria the number  $N_{\text{acc}}$  of events which pass these criteria is given by

$$N_{\text{acc}} = \mathcal{L} \sum_i \sigma_i \varepsilon_i + N_{\text{BG}}, \quad (1)$$

where  $N_{\text{BG}}$  is the number of beam-gas events,  $\mathcal{L}$  the integrated luminosity,  $\sigma_i$  and  $\varepsilon_i$  are the cross sections and corresponding hadron selection efficiencies for all colliding beam  $e^+e^-$  processes. The  $\sigma_i$  and  $\varepsilon_i$  are determined by Monte Carlo simulations of the relevant processes. It turns out that it is possible to vary cuts such that we can obtain a substantially larger fraction of beam-gas events in our hadronic data sample without large changes in the efficiencies. For such modified selection criteria we obtain

$$N'_{\text{acc}} = \mathcal{L} \sum_i \sigma_i \varepsilon'_i + r N_{\text{BG}}, \quad (2)$$

where  $r$  is the acceptance ratio for beam-gas events for the two sets of cuts. This factor  $r$  is determined using single beam data. Subtracting (1) from (2) we get

$$\Delta N_{\text{acc}} \equiv N'_{\text{acc}} - N_{\text{acc}} = \mathcal{L} \sum_i \sigma_i \Delta \varepsilon_i + (r-1) N_{\text{BG}}. \quad (3)$$

Since  $r$  is large and the change in the efficiencies  $\Delta \varepsilon$  is small, the change in the number of accepted events  $\Delta N_{\text{acc}}$  is fairly insensitive to the cross sections used. Solving (3) for  $N_{\text{BG}}$  gives the number of beam-gas events.

Both methods give consistent results. Taking the average we find that beam-gas background contributes only a very small fraction to the hadronic data sample from the continuum process  $e^+e^- \rightarrow \text{hadrons}$ :

$$f_{\text{BG}} \equiv N_{\text{BG}}/N_{\text{acc}} = (0.30 \pm 0.01 \pm 0.03)\%.$$

The first error is the statistical error. It is determined from the second method and reflects the statistics of the data used. The systematic error is derived from the difference in  $f_{\text{BG}}$  values obtained by both methods. For the  $Y$  scans  $f_{\text{BG}}$  is higher by a factor of 2 due to larger machine background. The distribution of this background as a function of c.m. energy is flat within statistical errors.

## 6 Luminosity measurement

The luminosity is measured using the  $e^+e^- \rightarrow e^+e^- (\gamma)$  and  $e^+e^- \rightarrow \gamma\gamma(\gamma)$  events observed in the main NaI(Tl) detector. Events which have exactly two energy clusters each with  $E_{\text{cluster}} > 0.35W$  and with directions inside  $|\cos\theta| < 0.75$ , are selected as luminosity events. The integrated luminosity  $\mathcal{L}$  is calculated from the number of luminosity events  $N_{\text{Lumi}}$  using

$$\mathcal{L} = N_{\text{Lumi}} W^2 / a. \quad (4)$$

The explicit energy factor  $W^2$  removes the *leading*  $1/W^2$  cross section dependence, allowing use of a constant conversion factor  $a$  within our limited  $W$  range. The value of  $a$  is determined by generating a sample of  $e^+e^- (\gamma)$  and  $\gamma\gamma(\gamma)$  Monte Carlo events with the program of Berends and Kleiss [7] and passing them through the full detector simulation as described in Sect. 4. The luminosity is corrected for the direct  $Y \rightarrow e^+e^-$  decays which contribute to  $N_{\text{Lumi}}$ .

A 2.5% systematic error on the luminosity is obtained by adding quadratically contributions from the following sources: 1.0% from Monte Carlo statistics, 1.0% from 4<sup>th</sup> order QED corrections [12], 1.9% from a variation of cuts within reasonable limits, 0.7% from the correction for direct decays  $Y \rightarrow e^+e^-$ , 0.2% from hadronic and beam-gas background, 0.1% from the *non-leading* energy dependence of the conversion factor  $a$ .

## 7 Radiative corrections and definition of $\Gamma_{ee}$

The measured excitation curve  $\sigma(W)$  of the resonance in the process  $e^+e^- \rightarrow Y \rightarrow \text{hadrons}$  is used to obtain  $\Gamma_{ee}$ . Without QED radiative corrections the cross section for the formation of the  $Y$  in  $e^+e^-$  annihilation has a Breit-Wigner form of width  $\Gamma_{\text{tot}}$ . For the  $Y(1S)$  and  $Y(2S)$ ,  $\Gamma_{\text{tot}}$  is about two orders of magnitude smaller than the r.m.s. spread  $\Delta$  in the c.m. energy of the storage ring due to synchrotron radiation, which for DORIS II is  $\Delta \approx 8$  MeV. Thus the Breit-Wigner can be safely approximated by a *delta* func-

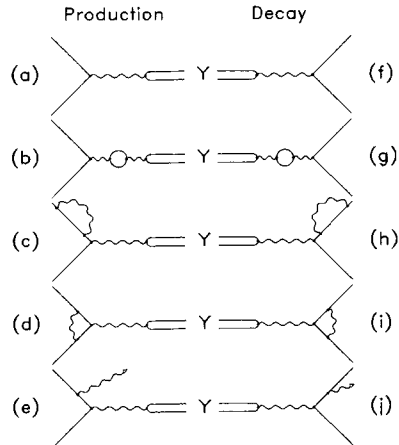


Fig. 3a–j. Feynman diagrams which contribute to  $\mathcal{O}(\alpha^3)$  to  $e^+e^- \rightarrow Y$  and  $Y \rightarrow e^+e^-$ . To this order the graphs **b**, **c**, **d** and **g**, **h**, **i** contribute only through their interference with the lowest order graphs **a** and **f**

tion,  $\sigma_{\text{BW}} = A^{(0)} \delta(W - M)$ , with  $A^{(0)}$  the area of the Breit-Wigner and  $M$  the mass of the resonance:

$$A^{(0)} = \frac{6\pi^2}{M^2} \Gamma_{ee}^{(0)} B_{\text{had}} \quad (5)$$

where  $B_{\text{had}}$  is the resonance branching ratio into hadrons. Convoluting this  $\delta$  function with the Gaussian distribution of the beam energy gives the effective lowest-order cross section:

$$\sigma^{(0)}(W) = A^{(0)} \frac{\exp(-z^2/2)}{\Delta \sqrt{2\pi}}, \quad z \equiv \frac{W - M}{\Delta}. \quad (6)$$

The  $^{(0)}$  in these equations indicate that the quantities are to lowest order in QED, corresponding to the Feynman graph of Fig. 3a. The  $\sigma^{(0)}(W)$  must then be multiplied by our efficiency for detecting hadronic events to get the observed cross section; this factor is discussed in Sect. 8.1. Here we are concerned with the QED radiative corrections to the *production* cross section  $\sigma^{(0)}(W)$ . They change both its shape and its normalization. The relevant Feynman diagrams to  $\mathcal{O}(\alpha^3)$  are shown in Fig. 3b–e.

Radiative corrections were initially calculated by Yennie et al. [13] and Bonneau and Martin [17]. Several other theoretical calculations have appeared since [18–20, 22, 30]. Generally, the result is a convolution of the lowest order cross section  $\sigma^{(0)}(W)$  with a distribution function which mainly reflects a bremsstrahlung energy spectrum. The result is of the form

$$\sigma(W) = A^{(0)} \frac{\exp(-z^2/4)}{\Delta \sqrt{2\pi}} N(z). \quad (7)$$

Most previous measurements of  $\Gamma_{ee}$  have used the functional forms for  $N(z)$  as obtained by Jackson and Scharre [18] or by Greco et al. [19], respectively:

$$N_{\text{JS}}(z) = \left(\frac{2\Delta}{W}\right)^t \Gamma(1+t) D_{-t}(-z) + (\delta_e + 2\Pi) \exp(-z^2/4), \quad (8a)$$

$$N_{\text{GPS}}(z) = \left(\frac{2\Delta}{W}\right)^t \Gamma(1+t) D_{-t}(-z) \cdot (1 + \delta_e + 2\Pi). \quad (8b)$$

Here  $\Gamma$  denotes the gamma function and  $D_{-t}$  is Weber's parabolic cylinder function [23]. Note that in the limit  $t \rightarrow 0$ ,  $D_{-t}(-z) \rightarrow \exp(-z^2/4)$  and the Gaussian shape of the machine resolution is recovered.

In the above formulae  $\delta_e = \frac{3}{4}t + \frac{2\alpha}{\pi} \left(\frac{\pi^2}{3} - \frac{1}{2}\right)$  stems from the vertex correction (Fig. 3d), and  $t = \frac{2\alpha}{\pi} \left(2 \ln \frac{W}{m_e} - 1\right)$  is the equivalent radiator thickness.  $\Pi$  is the vacuum polarization correction from the diagram of Fig. 3b. It includes the effect of all the lepton and quark loops in 3b:  $\Pi = \Pi_e + \Pi_\mu + \Pi_\tau + \Pi_{\text{quarks}}$ . The electron loop contributes  $\Pi_e = \frac{\alpha}{\pi} \left(\frac{2}{3} \ln \frac{W}{m_e} - \frac{5}{9}\right) \approx 0.014$  at energies  $W$  near the  $Y$  resonances. Muon and tau loops are calculated with their corresponding masses [20]. The quark loop contributions have been estimated by Berends and Komen [16] from the measured  $\sigma(e^+e^- \rightarrow \text{hadrons})$  to be  $\Pi_{\text{quarks}} \approx 0.017$ . Summing all fermion loop contributions yields  $\Pi \approx 0.038$  at our energy. In their original papers, Jackson and Scharre and Greco et al. ignored the  $\mu$ ,  $\tau$ , and quark contributions. In (8) we have corrected this by replacing  $\Pi_e$  by  $\Pi$  in their formulae.

Both forms of  $N(z)$  take into account the effect of many soft photons emission via "soft photon exponentiation", which leads to the  $(2\Delta/W)^t$  factors in (8). Jackson and Scharre apply it only to part of the cross section, whereas Greco et al. correct the entire  $\mathcal{O}(\alpha^3)$  expression. The difference is of  $\mathcal{O}(\alpha^4)$ , so that a definitive decision on which treatment is more accurate can only be made on the basis of a complete calculation to that order. Such a calculation has recently been done by Berends et al. [30], indicating good agreement with the form  $N_{\text{GPS}}(z)$ .

Thus  $N_{\text{GPS}}(z)$  is suitable for use with (5) and (7) to measure  $\Gamma_{ee}^{(0)} B_{\text{had}}$ . However, we are interested in the physical  $\Gamma_{ee}$ , corresponding to a calculation to all orders in  $\alpha$ .  $\Gamma_{ee}$  is defined as the partial width of

the decay  $Y \rightarrow e^+e^-$ . In QED  $Y \rightarrow e^+e^-$  is always accompanied by an infinite number of low energy photons. To avoid specifying a photon energy cut-off in measurements of  $B_{ee}$  (or  $B_{\mu\mu}$ ), it is conventional to include all decays with extra photons  $Y \rightarrow e^+e^- + n\gamma$  in the definition of  $\Gamma_{ee}$ . In order to relate  $\Gamma_{ee}$  to  $\Gamma_{ee}^{(0)}$ , we assume that the  $\mathcal{O}(\alpha^3)$  calculation is a good approximation to  $\Gamma_{ee}$ . The full set of diagrams contributing to the decay to  $\mathcal{O}(\alpha^3)$  are shown in Fig. 3f-j.  $\Gamma_{ee}^{(0)}$  corresponds to the lowest order diagram 3f alone. By the Kinoshita-Lee-Nauenberg theorem [14], the mass singularities from the vertex correction and the bremsstrahlung graphs (i.e. the terms proportional to  $\ln \frac{W}{m}$ ) cancel to each order in  $\alpha$ , leaving a finite part which is negligible [20]. Thus the only radiative correction which makes a net  $\mathcal{O}(\alpha^3)$  contribution to the decay comes from the vacuum polarization graph 3g interfering with the lowest order graph 3f. This leads to an increase of the partial width:

$$\Gamma_{ee} = (1 + 2\Pi) \Gamma_{ee}^{(0)}. \quad (9)$$

Lepton universality for  $\Gamma_{ll}^{(0)}$  implies  $\Gamma_{ee} \approx \Gamma_{\mu\mu} \approx \Gamma_{\tau\tau}$  to good approximation. Since  $1 + \delta_e + 2\Pi = (1 + \delta_e)(1 + 2\Pi)$  to this order in  $\alpha$ , we can remove the  $2\Pi$  from  $N(z)$  (8b) and introduce  $N'(z) = N(z)/(1 + 2\Pi)$ . This yields

$$\sigma(W) = A \frac{\exp(-z^2/4)}{\Delta \sqrt{2\pi}} N'(z) \quad (10)$$

with

$$A = \frac{6\pi^2}{M^2} \Gamma_{ee} B_{\text{had}}. \quad (11)$$

More recent calculations of the radiative corrections use this convention. Tsai [20] and Kuraev and Fadin [22] find, respectively:

$$N'_T(z) = \left(\frac{2\Delta}{W}\right)^T \Gamma(1+T) D_{-T}(-z) \cdot (1 - \Pi)^{-\delta_e T}, \quad (12a)$$

$$N'_{KF}(z) = \left(\frac{2\Delta}{W}\right)^t \Gamma(1+t) D_{-t}(-z) (1 + \delta_e). \quad (12b)$$

The  $N'_{KF}(z)$  is exactly  $N_{\text{GPS}}(z)$  with the  $2\Pi$  removed. In the expression of Tsai  $T = t \frac{1}{\Pi} \ln \left(\frac{1}{1 - \Pi}\right)$  is the equivalent radiator thickness corrected for pair production, which at  $W = M_{Y(1S)}$  differs from  $t$  by 0.32%. Some of the higher order corrections have also been calculated by Kuraev and Fadin, and differ from the renormalization group result of Tsai. However, the

results agree to  $\mathcal{O}(\alpha^3)$ . The above formula for  $N'_{KF}(z)$  omits the higher order terms.

Our results presented in Sect. 8 are based on the formalism of Kuraev and Fadin [22], using (10, 11, 12b) to obtain  $\Gamma_{ee} B_{\text{had}}$  directly. One could equally well use (5, 7, 8b) to obtain  $\Gamma_{ee}^{(0)} B_{\text{had}}$  and then apply (9) to get  $\Gamma_{ee} B_{\text{had}}$ . However, most previous measurements have used the formalism of Jackson and Scharre with  $\Pi = \Pi_e$ , resulting in something which is neither  $\Gamma_{ee}$  nor  $\Gamma_{ee}^{(0)}$ . A comparison with the results obtained using the various formalisms is presented in Sect. 9 to demonstrate the differences.

To obtain  $\Gamma_{ee}$  from  $\Gamma_{ee} B_{\text{had}}$  we need the hadronic branching ratio  $B_{\text{had}}$ . With the assumption that the resonance only decays into hadrons and lepton pairs we can use the relation  $B_{\text{had}} + 3 B_{\mu\mu} = 1$ . It is important to note that  $B_{\mu\mu}$  is measured including all extra photons in the decay and contains the vacuum polarization term from graph g of Fig. 3; otherwise the above equality would not hold. Also a determination of  $\Gamma_{\text{tot}} = \Gamma_{ee}/B_{\mu\mu}$  requires the vacuum polarization term to be included in the leptonic width [21].

## 8 $\Gamma_{ee}$ Measurements

The resonance parameters  $M$  and  $\Gamma_{ee}$  are determined by fitting the following function to the observed hadronic cross section:

$$\sigma^{\text{obs}}(W) = A^{\text{obs}} \frac{\exp(-z^2/4)}{\Delta\sqrt{2\pi}} N'_{KF}(z) + \frac{C}{W^2}. \quad (13)$$

The first term accounts for the decays  $Y \rightarrow \text{hadrons}$ .  $A^{\text{obs}} = A \varepsilon_H^R$  is the area of the Breit-Wigner multiplied by our hadronic detection efficiency for resonance decays. The resonance mass  $M$  enters by the variable  $z \equiv (W - M)/\Delta$ . Radiative corrections are treated according to the prescription of Kuraev and Fadin [22], using  $N'_{KF}(z)$  from (12b). The second term reflects hadron production from the continuum, which to lowest order scales as  $1/W^2$ . Over the narrow energy region used in the fits, the  $C/W^2$  continuum part of  $\sigma^{\text{obs}}(W)$  will include nearly all contributions from the background sources discussed in Sect. 5.

The data samples of hadronic events used for our  $\Gamma_{ee}$  determinations are summarized in Table 2. We have performed 4 scans over the  $Y(1S)$  resonance and one scan over the  $Y(2S)$ . Each scan has approximately  $100 \text{ nb}^{-1}$  per point. The value of  $\Gamma_{ee}$  determined from the scans is insensitive to small overall changes (of the order of  $\pm 10 \text{ MeV}$ ) in the absolute energy scale. It is, however, sensitive to the point-to-point error of the energy measurement.

**Table 2.** Data samples for the  $Y(1S)$  and  $Y(2S)$  scans and continuum data: energy range, number of hadronic events, total luminosity with statistical error, and number of data points

Scan	$W$ range [GeV]	# hadrons	$\sum \mathcal{L}$ [ $\text{nb}^{-1}$ ]	# points
<i>Y(1S) scans</i>				
1	9.388–9.506	12195	$2204 \pm 12$	21
2	9.445–9.477	6032	$690 \pm 7$	9
3	9.436–9.481	4008	$567 \pm 6$	7
4	9.444–9.479	5139	$670 \pm 7$	8
Total		27374	$4131 \pm 17$	45
<i>Y(2S) scan</i>				
	9.966–10.039	4367	$994 \pm 9$	10
<i>Continuum data</i>				
	9.39	25825	$7135 \pm 22$	

The most precise beam energy measurement at  $e^+e^-$  storage rings can be made by using a depolarization technique [24], if the beams are polarized. Due to the emission of synchrotron radiation electron and positron beams become polarized via the Sokolov-Ternov effect [25]. DORIS II provides a beam polarization of up to 80% in the  $Y(2S)$  energy region thus allowing a very precise energy determination for our  $Y(2S)$  scan data:  $\sigma_E/E \sim 2 \times 10^{-5}$ . Details of this measurement can be found in [26].

In the  $Y(1S)$  energy region the beam polarization is destroyed completely by storage ring resonances specific to the DORIS II machine configuration. Here the most precise measure of the relative beam energy comes from the determination of the magnetic field  $B$  at the beam position of a storage ring bending magnet using the nuclear magnetic resonance effect. The accuracy achieved here is  $\sigma_B/B \sim 5 \times 10^{-5}$ .

The determination of the beam energy from the magnetic field measurement depends on the machine parameters, which change with time, and on the degree of saturation of the magnets, which depends on the history of energy changes. We observe shifts of order 10 MeV between different run periods, and smaller shifts between successive scans. To avoid as much as possible a shift during a scan we always scan with monotonically increasing beam energy and complete each scan within a period of a few days, during which the machine parameters are held as constant as possible. The point-to-point error on the c.m. energy is taken from  $\sigma_B/B \sim 5 \times 10^{-5}$  to be 0.5 MeV. Although  $\Gamma_{ee}$  is nearly unaffected by small uncertainties in the absolute energy scale (of order  $\pm 10 \text{ MeV}$ ), we avoid any systematic influence from this effect by choosing the normalization factor between energy

and magnetic field so that the fitted resonance mass is equal to the nominal mass  $M_{Y(1S)} = 9460.0 \pm 0.2$  MeV [27]. For the limited energy range of our scans the beam energy is a linear function of the magnetic field  $B$ .

### 8.1 $\Gamma_{ee}$ of the $Y(1S)$

We first fit each scan individually to the function (13) with four free parameters:  $A^{\text{obs}}$ ,  $\Delta$ ,  $M$  and  $C$ . The values of  $A^{\text{obs}}$  and  $\Delta$  from these fits are labelled “ $C$  free” in Table 3. Only scan number 1 covers a wide enough  $W$  range for a good determination of the continuum constant  $C$ . Then we fit scans 2 to 4 with  $C$  fixed to the result obtained from scan 1. This results in the  $A^{\text{obs}}$  values labelled “ $C$  fixed” in Table 3. They agree within errors, but are not statistically independent and cannot simply be averaged to improve the statistical accuracy.

For our final result we fit the four scans simultaneously, allowing relative energy shifts between them as 3 additional free parameters. This makes maximum use of the continuum information and gives a statistically correct average of  $A^{\text{obs}}$ . The result of this fit, with the data of each scan corrected for its relative energy shift, is shown in Fig. 4. The  $\chi^2$  of 45.4 for 37 degrees of freedom corresponds to a confidence level of 16.1%. The parameter values are:  $A^{\text{obs}} = 286 \pm 6$  nb MeV,  $\Delta = 7.8 \pm 0.2$  MeV, and  $C = 300 \pm 6$  nb GeV<sup>2</sup>. Scans 2, 3 and 4 are shifted in nominal c.m. energy from scan 1 by  $-4.0 \pm 0.4$  MeV,  $-8.6 \pm 0.4$  MeV,  $-7.8 \pm 0.4$  MeV, respectively. The machine resolution  $\Delta$  is compatible with the expected value of 7.6 MeV.

$\Gamma_{ee} B_{\text{had}}$  is calculated from (11) and  $A = A^{\text{obs}} / \varepsilon_H^R$  where  $\varepsilon_H^R$  is the probability that a resonance decay is accepted in our hadronic sample. To obtain  $\varepsilon_H^R$  Monte Carlo techniques as described in Sect. 4 are used. With the standard LUND program version 6.2 [3] we generate the following  $Y(1S)$  decay modes with

**Table 3.** Results of fits to  $Y(1S)$  scans. Errors are statistical only.  $CL$  is the confidence level of the particular fit

Scan	$A^{\text{obs}}$ [nb MeV]	$\Delta$ [MeV]	$C$ [nb GeV <sup>2</sup> ]	$CL$ [%]	Comment
1	$289 \pm 8$	$7.7 \pm 0.3$	$300 \pm 6$	14.2	$C$ free
2	$269 \pm 32$	$7.2 \pm 0.6$	$327 \pm 48$	74.3	$C$ free
3	$312 \pm 19$	$8.3 \pm 0.5$	$280 \pm 20$	4.0	$C$ free
4	$221 \pm 21$	$6.8 \pm 0.6$	$374 \pm 31$	32.9	$C$ free
2	$288 \pm 9$	$7.5 \pm 0.3$	300	81.6	$C$ fixed
3	$298 \pm 11$	$7.9 \pm 0.3$	300	6.2	$C$ fixed
4	$271 \pm 9$	$8.0 \pm 0.3$	300	12.8	$C$ fixed

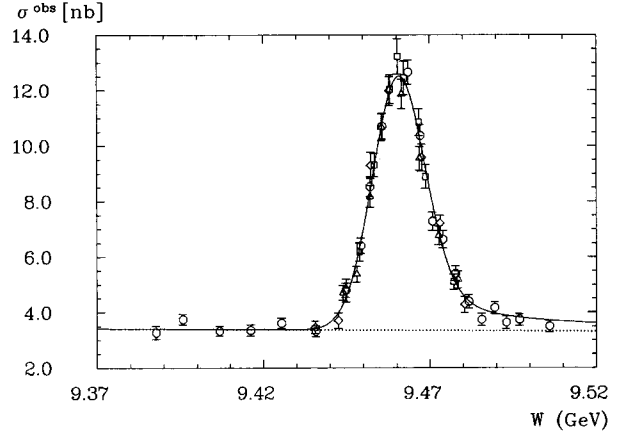


**Fig. 4.** Observed cross section vs. c.m. energy  $W$  for the four  $Y(1S)$  scans. Circles represent scan 1, squares scan 2, triangles scan 3, and diamonds scan 4. The full line is the fit result; the dotted line shows the fitted background

**Table 4.** Summary of hadronic detection efficiencies for  $Y(1S)$  and  $Y(2S)$  decays and for the continuum process  $e^+e^- \rightarrow \text{hadrons}$ . The errors are from Monte Carlo statistics only

Efficiency symbol	Process	$W$ [GeV]	$\varepsilon$ [%]	Comments
$\varepsilon_H^{Y(1S)}$	$Y(1S) \rightarrow \text{hadrons}$	9.46	$83.1 \pm 0.1$	unpol. beams
$\varepsilon_H^{Y(2S)}$	$Y(2S) \rightarrow \text{hadrons}$	10.02	$85.4 \pm 0.2$	80% beam pol.
$\varepsilon_{q\bar{q}}^{\text{Cont}}$	$e^+e^- \rightarrow q\bar{q}$	9.39	$72.0 \pm 0.5$	unpol. beams

branching ratios according to the Particle Data Group values [27]: a) decays into 3 gluons and  $\gamma gg$ ; b) direct decays to  $q\bar{q}$ ; c) decays into two leptons. Typical detection efficiencies for the  $Y$  resonances are a)  $\varepsilon_{3g}^Y = 90\%$ , b)  $\varepsilon_{q\bar{q}}^Y = 80\%$ , c)  $\varepsilon_{\tau^+\tau^-}^Y = 15\%$ , whereas  $\varepsilon_{e^+e^-}^Y$  and  $\varepsilon_{\mu^+\mu^-}^Y$  are negligibly small. We get as total detection efficiency  $\varepsilon_H^{Y(1S)} = 83.1 \pm 0.1 \pm 2.4\%$  (see Table 4). The first error results from Monte Carlo statistics, whereas the second systematic error originates from the hadronization model used and the detector response. We find a 1.4% difference in the efficiency using the standard LUND string fragmentation and a coherent parton shower model. In addition we estimate a 2.5% systematic error to account for uncertainties in modelling the detector response.

Using the measured value of  $A^{\text{obs}}$  and  $\varepsilon_H^{Y(1S)}$  we obtain

$$\Gamma_{ee} B_{\text{had}} = 1.23 \pm 0.02 \pm 0.05 \text{ keV}. \quad (14)$$

The 4.1% systematic error is explained in Sect. 8.3. Division by  $B_{\text{had}} = 1 - 3B_{\mu\mu}$  using the world average of  $B_{\mu\mu}(Y(1S)) = (2.63 \pm 0.12)\%$  from Table 5 yields

$$\Gamma_{ee} = 1.34 \pm 0.03 \pm 0.06 \text{ keV}. \quad (15)$$



**Table 5.** Compilation of  $B_{\mu\mu}$  values (in %) for  $\Upsilon(1S)$  and  $\Upsilon(2S)$  and world averages

Reaction	$B_{\mu\mu}$	Experiment
$\Upsilon(1S)$		
$\Upsilon \rightarrow \mu\mu$	$2.2 \pm 2.0$	PLUTO [41]
$\Upsilon \rightarrow \mu\mu$	$1.4^{+3.4}_{-1.4}$	DESY-Heid. [31]
$\Upsilon \rightarrow \mu\mu$	$3.2 \pm 1.3 \pm 0.3$	DASP II [33]
$\Upsilon \rightarrow \mu\mu$	$3.8 \pm 1.5 \pm 0.2$	LENA [32]
$\Upsilon \rightarrow \mu\mu$	$2.7 \pm 0.3 \pm 0.3$	CLEO [46]
$\Upsilon \rightarrow \mu\mu$	$2.7 \pm 0.3 \pm 0.1$	CUSB [47]
$\Upsilon \rightarrow ee$	$5.1 \pm 3.0$	PLUTO [48]
$\Upsilon(2S) \rightarrow \pi^+ \pi^- \Upsilon$	$2.84 \pm 0.18 \pm 0.20$	CLEO [42]
$\Upsilon$		
$\rightarrow \mu^+ \mu^-, e^+ e^-$		
$\Upsilon(2S) \rightarrow \pi^+ \pi^- \Upsilon$	$2.39 \pm 0.12 \pm 0.14$	ARGUS [49]
$\Upsilon$		
$\rightarrow \mu^+ \mu^-, e^+ e^-$		
$\Upsilon \rightarrow \tau\tau$	$3.4 \pm 0.4 \pm 0.4$	CLEO [43]
	$2.63 \pm 0.12$	average
$\Upsilon(2S)$		
$\Upsilon(2S) \rightarrow \mu\mu$	$1.8 \pm 0.8 \pm 0.5$	CLEO [44]
$\Upsilon(2S) \rightarrow \mu\mu$	$1.4 \pm 0.3 \pm 0.2$	CUSB [47]
$\Upsilon(2S) \rightarrow \mu\mu$	$1.0 \pm 0.6 \pm 0.5^a$	ARGUS [45]
$\Upsilon(2S) \rightarrow \tau\tau$	$1.7 \pm 1.5 \pm 0.6$	CLEO [44]
	$1.4 \pm 0.3$	average

<sup>a</sup> The ARGUS  $\Upsilon(2S)$  value is scaled from the average  $\Upsilon(1S)$  value with  $B_{\mu\mu}(2S) = 1.57 \pm 0.59 \pm 0.53 + 2.1(B_{\mu\mu}(1S) - 2.9)$  (in %) [45]

## 8.2 $\Gamma_{ee}$ of the $\Upsilon(2S)$

For the scan over the  $\Upsilon(2S)$  we have the  $\sigma_E \approx 0.2$  MeV energy determination for each scan point from depolarization measurements. Fitting our data as a function of energy to the expression of (13) gives the following results for the parameters:  $M = 10023.5 \pm 0.4$  MeV in agreement with our published value [26] and that of [27],  $A^{\text{obs}} = 110 \pm 8$  nb MeV,  $\Delta = 8.2 \pm 0.5$  MeV which agrees with the expected machine resolution of 8.5 MeV at  $M_{\Upsilon(2S)}$ , and  $C = 296 \pm 12$  nb GeV<sup>2</sup>, compatible with the value found at the  $\Upsilon(1S)$ . The fit has a  $\chi^2$  of 12.5 for 5 degrees of freedom corresponding to a 2.8% confidence level. The data and the resulting fit curve are shown in Fig. 5.

The Monte Carlo event sample used to determine the hadronic detection efficiency for the  $\Upsilon(2S)$  includes in addition to the decay channels considered for the  $\Upsilon(1S)$  the following decay modes: d) radiative decays to the three  $^3P_{0,1,2}$  states which in turn either decay radiatively to the  $\Upsilon(1S)$  or via 2 gluons ( $^3P_0, ^3P_2$ ) or 3 gluons ( $^3P_1$ ); e)  $\pi^+ \pi^-$  and  $\pi^0 \pi^0$  transitions to the  $\Upsilon(1S)$ . The events were generated with a beam polarization of 80% as observed in our data. We obtain a detection efficiency (see Table 4) of

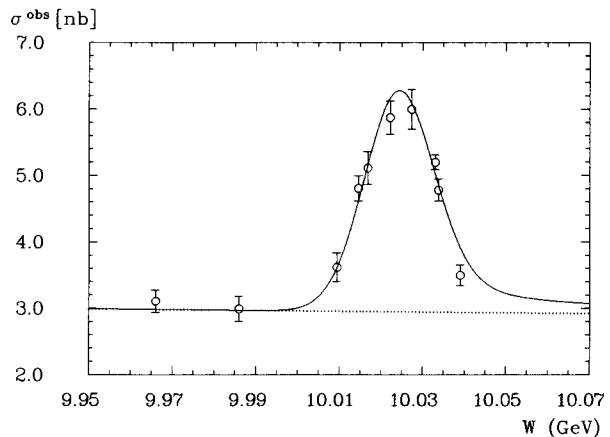


**Fig. 5.** Observed cross section vs. c.m. energy  $W$  for the  $\Upsilon(2S)$  scan. The full line is the fit result, the dotted line shows the fitted background

$\epsilon_H^{\Upsilon(2S)} = 85.4 \pm 0.2 \pm 2.5\%$  with statistical and systematic errors as discussed for the  $\Upsilon(1S)$  in Sect. 8.1. Using this value, the measured value of  $A^{\text{obs}}$  and  $B_{\mu\mu} = (1.4 \pm 0.3)\%$  from Table 5 we obtain

$$\Gamma_{ee} B_{\text{had}} = 0.54 \pm 0.04 \pm 0.02 \text{ keV} \quad (16)$$

and

$$\Gamma_{ee} = 0.56 \pm 0.04 \pm 0.02 \text{ keV}. \quad (17)$$

## 8.3 Systematic errors for $\Gamma_{ee}$

One of the largest contributions to the systematic error comes from the 2.5% uncertainty in the luminosity determination.

A 2.8% systematic error on the detection efficiencies for the  $\Upsilon(1S)$  and the  $\Upsilon(2S)$  is the quadratic sum of the contributions already discussed in Sect. 8.1.

We allow a 1.5% error for the dependence on cuts, found by varying them within acceptable limits, and by using an alternate hadron selection method described in [29].

Next we consider the effect of backgrounds in our data sample. Background contributions from the continuum QED processes  $e^+ e^- \rightarrow e^+ e^-, \gamma\gamma, \mu^+ \mu^-,$  and  $\tau^+ \tau^-$  are already suppressed by our event selection. Moreover, the lowest order cross sections for these processes all scale like  $1/W^2$ , so that events of this type are mostly included in the  $C/W^2$  term. The determination of the area  $A^{\text{obs}}$  under the resonance curve is not affected by background contributions. In Sect. 5.3 we estimate the beam-gas contamination to be 0.6%. This background has a flat distribution as a function of energy and is almost completely absorbed in the continuum term  $C/W^2$  of (13). Two-

photon reactions have a cross section proportional to  $\ln W^2$ , as do higher-order corrections to the continuum QED background. To check for any such background we also perform fits to the data adding a second background term  $C' \ln W^2$  to (13). These fits give  $C' = 0 \pm 3$  nb,  $C = 300 \pm 10$  nb GeV<sup>2</sup>. The latter value is the same as obtained in Sect. 8 without the  $\ln W^2$  term. Also all other fitted parameter are completely unaffected by adding such a term. Over the scanned energy range, the value found for  $C'$ , which is highly anticorrelated with  $C$ , would result in a 0.3% change (at the 1 S.D. level) of the background, if there were contributions from processes with energy dependence proportional to  $\ln W^2$ .

To test for possible c.m. energy shifts within each individual one of our scans we make several additional fits to them. Between any two scan points we split each scan in two parts allowing as an additional fit parameter an energy shift of one part with respect to the other. Within errors the fitted single shifts are always compatible with zero. The probability that *all* shifts together are zero is as high as 31%. Again within errors the fitted  $A^{\text{obs}}$  do not deviate from the values given in Sect. 8 obtained without any shift.

Combining the errors quadratically we obtain a 4.1% systematic error on our  $\Gamma_{ee} B_{\text{had}}$  values. Dividing by  $1-3 B_{\mu\mu}$  to obtain  $\Gamma_{ee}$  introduces an additional systematic error of 0.4% for the  $\Upsilon(1S)$  and of 1.3% for the  $\Upsilon(2S)$ .

## 9 Discussion of $\Gamma_{ee}$ results

Previous measurements of  $\Gamma_{ee}$  of the  $\Upsilon$ 's used either the Jackson-Scharre or the Greco et al. formulation of radiative corrections, which differ from the Kuraev-Fadin form we used, as discussed in Sect. 7. However, all of the forms in (8 and 12) give very similar shapes, with differences appearing in the normalization. Thus previous measurements can be renormalized to correspond to the Kuraev-Fadin formulation by comparing the values of  $N(z=0)$  in (8, 12). This is done in Table 6, and compared to our values. Here we compare  $\Gamma_{ee} B_{\text{had}}$  rather than  $\Gamma_{ee}$  to remove the dependence on  $B_{\mu\mu}$ , which was not very well known at the time of the earliest  $\Gamma_{ee}$  measurements. Adding the statistical and systematic errors in quadrature shows our result to be the most precise single measurement for the  $\Upsilon(1S)$  as well as for the  $\Upsilon(2S)$ . The agreement with the world averages, calculated without our values, is excellent.

Based on our data we give a comparison of  $\Gamma_{ee}$  values for the  $\Upsilon(1S)$  obtained applying the four different radiative corrections according to (8 and 12) in Fig. 6, the errors shown are statistical only. Although Tsai's ansatz [20] has been criticized by Kuraev and Fadin, both prescriptions give nearly the same  $\Gamma_{ee}$  result, since they are equal to the order of corrections considered here. The point marked as "Berends et al." shows the result using their  $\mathcal{O}(\alpha^4)$  calculation [30].

**Table 6.** Measurements of  $\Gamma_{ee} B_{\text{had}}$  (in keV). The type of radiative correction that was used in each published value is listed, and the rescaled value is given. KF: Kuraev and Fadin, JS: Jackson and Scharre, GPS: Greco et al.

Published $\Gamma_{ee} B_{\text{had}}$	Rad. corr.	Rescaled value	Experiment
$\Upsilon(1S)$			
$1.00 \pm 0.23$	JS	$1.09 \pm 0.25$	DESY-Heidelberg [31]
$1.10 \pm 0.07 \pm 0.11$	GPS	$1.13 \pm 0.13$	LENA [32]
$1.12 \pm 0.07 \pm 0.04$	JS	$1.23 \pm 0.09$	DASP II [33]
$1.17 \pm 0.05 \pm 0.08$	JS, full $\Pi$	$1.37 \pm 0.11$	CLEO [34]
$1.04 \pm 0.05 \pm 0.09$	JS	$1.17 \pm 0.11$	CUSB [35] (unpub.)
		$1.22 \pm 0.05$	prev. average
	KF	$1.23 \pm 0.02 \pm 0.05$	this experiment
		$1.23 \pm 0.04$	new average
$\Upsilon(2S)$			
$0.37 \pm 0.16$	JS	$0.41 \pm 0.18$	DESY-Heidelberg [31]
$0.53 \pm 0.07^{+0.09}_{-0.05}$	GPS	$0.54 \pm 0.12$	LENA [32]
$0.55 \pm 0.11 \pm 0.06$	JS	$0.60 \pm 0.14$	DASP II [33]
$0.49 \pm 0.03 \pm 0.04$	JS, full $\Pi$	$0.58 \pm 0.06$	CLEO [34]
$0.53 \pm 0.03 \pm 0.05$	JS	$0.59 \pm 0.06$	CUSB [35] (unpub.)
		$0.57 \pm 0.04$	prev. average
	KF	$0.54 \pm 0.04 \pm 0.02$	this experiment
		$0.56 \pm 0.03$	new average

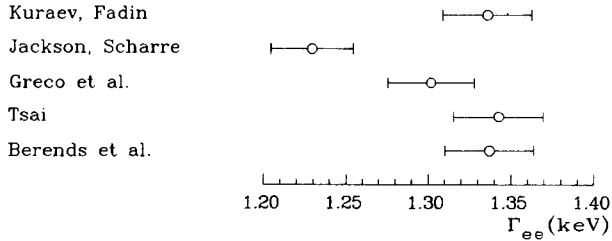


**Fig. 6.** Compilation of  $\Gamma_{ee}$  results for the  $Y(1S)$  obtained using different radiative corrections: Kuraev and Fadin [22], Jackson and Scharre [18], Greco et al. [19], Tsai [20], full  $\mathcal{O}(\alpha^4)$  calculation by Berends et al. [30]. The errors are statistical only

**Table 7.** Rescaling factors for  $\Gamma_{ee}$ . Ratios of  $N(z=0)$  compared to  $\Gamma_{ee}$  ratios from fits to our  $Y(1S)$  scans using different prescriptions for radiative corrections. The smallness of the errors on the measured ratios arises from the positive correlation of individual  $\Gamma_{ee}$  values. KF: Kuraev and Fadin, JS: Jackson and Scharre, GPS: Greco et al., T: Tsai

Radiative corrections	Ratio from $\Gamma_{ee}$	Ratio from $N(z=0)$
KF/JS	$1.08655 \pm 0.00010$	1.09340
KF/GPS	$1.02600 \pm 0.00002$	1.02600
KF/T	$0.99955 \pm 0.00003$	0.99911

Using the expressions of Jackson and Scharre [18], (8a), and of Greco et al. [19], (8b), the  $\Gamma_{ee}$  values are lower due to the inclusion of  $\Pi_e$ , the electronic vacuum polarization contribution. In Table 7 we compare ratios of  $N(z=0)$  to the corresponding ratios of  $\Gamma_{ee}$  values extracted from our  $Y(1S)$  scans using the various prescriptions. The agreement to better than 1% supports the applicability of the rescaling procedure.

## 10 Determination of $R$

The determination of  $R$  follows its traditional definition:  $R$  is the ratio of non-resonant hadronic cross section to the Born cross section of  $\mu$  pair production

$$R = \frac{\sigma^{(0)}(e^+e^- \rightarrow \text{hadrons})}{\sigma^{(0)}(e^+e^- \rightarrow \mu^+\mu^-)}. \quad (18)$$

In contrast to  $\Gamma_{ee}$ , which is a physical quantity,  $R$  is a theorist's ratio, in which the effect of QED corrections is removed, as indicated by the symbol  $\sigma^{(0)}$ . The lowest order  $\mu$  pair production cross section at fixed c.m. energy  $W$  is given by [27]

$$\sigma^{(0)}(e^+e^- \rightarrow \mu^+\mu^-) = \frac{4\pi}{3} \frac{\alpha^2}{W^2} = \frac{86.9}{W^2} \text{ nb GeV}^2. \quad (19)$$

We have  $\sim 7.1 \text{ pb}^{-1}$  of data (see Table 2) taken in the continuum below the  $Y(1S)$  at c.m. energy  $W=9.39 \text{ GeV}$ . The observed hadronic cross section  $\sigma^{\text{obs}}$  is given by  $N_{\text{hadrons}}$ , the number of selected hadronic events, and the luminosity  $\mathcal{L}$ :

$$\sigma^{\text{obs}} = \frac{N_{\text{hadrons}}}{\mathcal{L}}. \quad (20)$$

We define the quantity

$$\mathcal{C} = \sigma^{\text{obs}} W^2 \quad (21)$$

which is determined run by run. Taking the weighted average we obtain  $\mathcal{C} = 300.38 \pm 2.86 \text{ nb GeV}^2$ . Combining (19) with (21) gives the observed  $R^{\text{obs}}$ :

$$R^{\text{obs}} = \frac{\mathcal{C}}{86.9 \text{ nb GeV}^2}. \quad (22)$$

As discussed in detail in refs. [36] and [37],  $R$  is obtained from  $R^{\text{obs}}$  as follows:

$$R = \frac{R^{\text{obs}}(1 - f_{\text{BG}}) - \Delta R_{\text{QED}} - \Delta R_{\gamma\gamma}}{\varepsilon_{q\bar{q}}^{\text{Cont}}(1 + \delta_R)}. \quad (23)$$

$\delta_R$  accounts for the initial state radiative corrections,  $\delta_R = 0.291$  [37] at  $W=9.39 \text{ GeV}$ . Here a cut-off at 1% of the beam energy has been applied for the energy of bremsstrahlung photons.  $f_{\text{BG}} = 0.3\%$  is the percentage beam-gas contamination (see Sect. 5.3).  $\Delta R_{\text{QED}} = 0.187 \pm 0.005$  is the background at  $W=9.39 \text{ GeV}$  from the continuum QED processes  $e^+e^- \rightarrow e^+e^-$ ,  $\gamma\gamma$ ,  $\mu^+\mu^-$ , and  $\tau^+\tau^-$  which pass our hadron selection criteria.  $\Delta R_{\gamma\gamma} = 0.020 \pm 0.006$  is the background from two-photon collisions. The  $\Delta R$  are calculated from  $\varepsilon\sigma$  of Table 1 as  $\Delta R = \varepsilon\sigma W^2 / (86.9 \text{ nb GeV}^2)$ .  $\varepsilon_{q\bar{q}}^{\text{Cont}}$  is the detection efficiency for continuum hadron production. We use the average of the  $e^+e^- \rightarrow q\bar{q}$  efficiencies obtained with the standard LUND string fragmentation and the coherent parton shower model (see Table 4).

The systematic error on  $R$  receives contributions from the following sources: The 1.4% difference of the efficiencies for the LUND string and the coherent shower model is taken as systematic uncertainty resulting from the hadronization model used. We estimate a 2.5% systematic error to account for uncertainties in modelling the detector response. The error on the luminosity determination is 2.5%. The backgrounds which have to be subtracted are already small due to our selection cuts. The systematic error on the beam-gas fraction is  $\Delta f_{\text{BG}}/f_{\text{BG}} = 10\%$ . If we conservatively allow for a 5% systematic uncertainty in  $\Delta R_{\text{QED}}$  and if we assume that for two-photon background the cross sections of both, the GVDM and

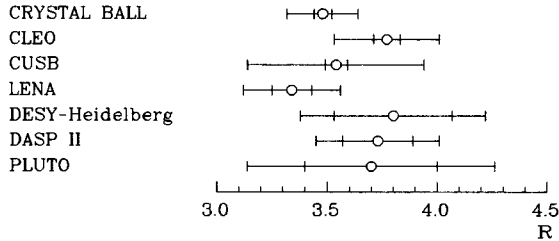


Fig. 7. Compilation of  $R$  values. The small error bars represent statistical, the large error bars systematic errors separately. The quoted values are measured at the following c.m. energies: CLEO [34]  $W=10.4$  GeV; CUSB [38]  $W=10.4$  GeV; LENA [28]  $W=9.30$  GeV; DESY-Heidelberg [31]  $W=9.45$  GeV; DASP II [39]  $W=9.5$  GeV; PLUTO [40]  $W=9.4$  GeV

QPM contributions are known only within a factor of 2, then the background subtraction affects our  $R$  by less than 0.6%. The dependence on hadron selection cuts is determined as described in Sect. 8.3 and contributes 2.5%. Finally, according to [37]  $\delta_R$  is known to 1%. The factor  $(1 + \delta_R)^{-1}$  thus gives another 0.1% systematic uncertainty. Adding the different contributions quadratically we assign a 4.6% systematic error to the measured  $R$  value. We then obtain

$$R = 3.49 \pm 0.05 \pm 0.16 \quad \text{at } W = 9.39 \text{ GeV},$$

where the errors are statistical and systematic, respectively.

As a cross check of this result we also determine  $R$  from the continuum contribution in our resonance scan data by the same method as discussed above. Here  $\mathcal{C}$  is the value of the continuum parameter  $C$  found in the fit to our  $Y(1S)$  scans:  $C = 300 \pm 6$  nb GeV<sup>2</sup>. We find

$$R = 3.47 \pm 0.07 \pm 0.16 \quad \text{at } W = 9.46 \text{ GeV}.$$

Both  $R$  values agree within statistical errors. The statistical error on the latter value is larger reflecting the smaller data sample. The systematic error is the same as discussed above.

The expected change in  $R$  when changing  $W$  from 9.39 GeV to 9.46 GeV is of the order of  $\Delta R/R \sim 10^{-4}$  and thus not observable within our accuracy. So taking the weighted average of the two measurements we obtain.

$$R = 3.48 \pm 0.04 \pm 0.16.$$

A compilation of  $R$  values in the energy range  $W=9.3$  to 10.4 GeV is given in Fig. 7. In this energy range no flavor threshold is crossed and changes in  $R$  due to the energy dependence of the strong coupling constant are unobservable within present statistics. Our

result agrees with most of the published values within statistical errors. Our systematic uncertainty is considerably smaller than for the other measurements.

## 11 Conclusions

With the Crystal Ball detector operating at the DORIS II storage ring we have measured the leptonic partial widths  $\Gamma_{ee}$  of the  $Y(1S)$  and  $Y(2S)$  resonances. Using the prescription of Kuraev and Fadin [22] to correct for initial state radiation, we find

$$\Gamma_{ee}(Y(1S)) = 1.34 \pm 0.03 \pm 0.06 \text{ keV}$$

and

$$\Gamma_{ee}(Y(2S)) = 0.56 \pm 0.04 \pm 0.02 \text{ keV}.$$

The errors are statistical and systematic, respectively. These values are the most precise single measurements, and agree well with the averages of previous measurements rescaled to the radiative corrections of Kuraev and Fadin. With these corrections the new world averages are

$$\Gamma_{ee}(Y(1S)) = 1.34 \pm 0.05 \text{ keV}$$

and

$$\Gamma_{ee}(Y(2S)) = 0.58 \pm 0.03 \text{ keV}.$$

To compare with theoretical predictions, the experimental  $\Gamma_{ee}$  values should be divided by 1.07 to include the effect of vacuum polarization [20, 21]. Using the current world averages for  $B_{\mu\mu}$  we obtain the total widths

$$\Gamma_{\text{tot}}(Y(1S)) = 51 \pm 4 \text{ keV}$$

and

$$\Gamma_{\text{tot}}(Y(2S)) = 40 \pm 9 \text{ keV}.$$

Finally, we determine  $R$ , the ratio of non-resonant hadronic cross section to the Born cross section of  $\mu$  pair production, at c.m. energy  $W=9.39$  GeV and find

$$R = 3.48 \pm 0.04 \pm 0.16.$$

Our value of  $R$  agrees within statistical errors with published results, and has the smallest systematic uncertainty.

*Acknowledgements.* We would like to thank the DESY and SLAC directorates for their support. This experiment would not have been possible without the dedication of the DORIS machine group as well as the experimental support groups at DESY. Those of us

from abroad wish to thank the DESY laboratory for the hospitality extended to us while working at DESY.

Z.J., B.M., and G.N. thank DESY for financial support. D.W. acknowledges support from the National Science Foundation. E.D.B., R.H., and K.S. have benefitted from financial support from the Humboldt Foundation. S.C. acknowledges support from the Dept. of Physics and Laboratory of Nuclear Science of the Massachusetts Institute of Technology. K.K. acknowledges support from the Heisenberg Foundation. The Nijmegen group acknowledges the support of FOM-ZWO. The Erlangen, Hamburg, and Würzburg groups acknowledge financial support from the German Federal Minister for Research and Technology (BMFT) under the contract numbers 054 ER 11P(5), 054 HH 11P(7), 054 WU 11P(1) and from the Deutsche Forschungsgemeinschaft (Hamburg). This work was supported in part by the U.S. Department of Energy under Contract No. DE-AC03-81ER40050 (CIT), No. DE-AC02-76ER03066 (CMU), No. DE-AC02-76ER03064 (Harvard), No. DE-AC02-76ER03072 (Princeton), No. DE-AC03-76SF00515 (SLAC), No. DE-AC03-76SF00326 (Stanford), and by the National Science Foundation under Grants No. PHY75-22980 (CIT), No. PHY81-07396 (HEPL), No. PHY82-08761 (Princeton).

## References

1. R. Herb et al.: Phys. Rev. Lett. 39 (1977) 252
2. E.D. Bloom, C.W. Peck: Ann. Rev. Nucl. Part. Sci. 33 (1983) 143; Crystal Ball Collab. M. Oreglia et al.: Phys. Rev. D 25 (1982) 2259
3. T. Sjöstrand: Lund preprint, LU TP 85-10, 1985; T. Sjöstrand, M. Bengtsson: Comput. Phys. Commun. 43 (1987) 367
4. B.R. Webber: Nucl. Phys. B 238 (1984) 492; G. Marchesini, B.R. Webber: Nucl. Phys. B 238 (1984) 1
5. R. Ford, W. Nelson: SLAC-210 (1978), unpublished
6. H. Fesefeldt: Aachen preprint, PITHA 85/02, unpublished
7. F.A. Berends, R. Kleiss: Nucl. Phys. B 228 (1983) 537; Nucl. Phys. B 186 (1981) 22
8. F.A. Berends, R. Kleiss, S. Jadach, Z. Wąs: Acta Phys. Pol. B 14 (1983) 413
9. S.L. Cartwright: Proc. 6th Int. Conf. on Physics in Collision (Chicago, 1986)
10. J.M. Vermaseren: Nucl. Phys. B 229 (1983) 347; G.P. Lepage: J. Comp. Phys. 27 (1978) 192
11. R.H. Dalitz, D.R. Yennie: Phys. Rev. 105 (1957) 1598
12. B. Naroska: Phys. Rep. 148 (1987) 98
13. D.R. Yennie, S.C. Frautschi, H. Suura: Ann. Phys. 13 (1961) 379
14. T. Kinoshita: J. Math. Phys. 3 (1962) 650; T.D. Lee, M. Nauenberg: Phys. Rev. 133 (1964) B 1549
15. The most explicit discussion of the procedure how to measure  $B_{\mu\mu}$  can be found in [46]
16. F.A. Berends, G.J. Komen: Phys. Lett. 63 B (1976) 432
17. G. Bonneau, F. Martin: Nucl. Phys. B 27 (1971) 381
18. J.D. Jackson, D.L. Scharre: Nucl. Instrum. Methods 128 (1975) 13
19. M. Greco, G. Pancheri-Srivastava, Y. Srivastava: Phys. Lett. 56 B (1975) 367
20. Y.S. Tsai: SLAC-PUB-3129 (1983), unpublished
21. K. Königsmann: Proc. 6th Int. Conf. on Physics in Collision (Chicago, 1986) and DESY 86-136 (1986); W. Buchmüller, S. Cooper: MIT preprint MIT-LNS-159 (1987); J.P. Alexander et al.: SLAC-PUB-4501 (1988), submitted to Nucl. Phys.
22. E.A. Kuraev, V.S. Fadin: Sov. J. Nucl. Phys. 41 (1985) 466
23. M. Abramowitz, I.A. Stegun: Handbook of mathematical functions. New York: Dover 1972
24. S.I. Serednyakov et al.: JETP 44 (1976) 1063; R. Neumann, R. Rosmanith: Nucl. Instrum. Methods 204 (1982) 29
25. A.A. Sokolov, I.M. Ternov: Sov. Phys. Dokl. 18 (1964) 1203
26. ARGUS Collab. and Crystal Ball Collab. D.P. Barber et al.: Phys. Lett. 135 B (1984) 498
27. Particle Data Group M. Aguilar-Benitez et al.: Phys. Lett. 170 B (1986) 1
28. LENA Collab. B. Niczyporuk et al.: Z. Phys. C – Particles and Fields 15 (1982) 299
29. Crystal Ball Collab. A. Osterheld et al.: SLAC-PUB-4160 (1987), submitted to Phys. Rev. D
30. F.A. Berends, G.J.H. Burgers, W.L. Van Neerven: Phys. Lett. 185 B (1987) 395
31. DESY-Heidelberg Collab. P. Bock et al.: Z. Phys. C – Particles and Fields 6 (1980) 125
32. LENA Collab. B. Niczyporuk et al.: Phys. Rev. Lett. 46 (1981) 92; Phys. Lett. 99 B (1981) 169. In [28], this group revised their  $\Gamma_{ee}(1S)$  value, normalizing to their new measurement of the continuum  $R$ . However, the  $R$  they originally used is closer to the current average  $R$ , see [34]; therefore we use their original  $\Gamma_{ee}$ . They used a modified Jackson-Scharre radiative corrections, which correspond to the Greco form given here as (8b) (B. Niczyporuk, private communication)
33. DASP II Collab. H. Albrecht et al.: Phys. Lett. 116 B (1982) 383
34. CLEO Collab. R. Giles et al.: Phys. Rev. D 29 (1984) 1285. The values for  $\Gamma_{ee} B_{\text{had}}$  before correction for  $B_{\mu\mu}$  are quoted in [46]. The value of  $2\mathcal{I}_{\text{quarks}}$  used is 0.034, as quoted in R.K. Plunkett, Cornell Ph. D. Thesis (1983)
35. P.M. Tuts: Proc. Int. Symp. on Lepton and Photon Interactions at High Energy, Ithaca, N.Y. (1983) and private communication
36. R.M. Barnett, M. Dine, L. McLerran: Phys. Rev. D 22 (1980) 594
37. F.A. Berends, R. Kleiss: Nucl. Phys. B 178 (1981) 141
38. CUSB Collab. E. Rice et al.: Phys. Rev. Lett. 48 (1982) 906
39. DASP II Collab. H. Albrecht et al.: Phys. Lett. 116 B (1982) 383
40. PLUTO Collab. Ch. Berger et al.: Phys. Lett. 81 B (1979) 410. The CLEO Collaboration [34] quotes a value of  $R = 3.67 \pm 0.23 \pm 0.29$  from PLUTO Collab. Ch. Berger et al.: Phys. Lett. 76 B (1978) 243
41. PLUTO Collab. Ch. Berger et al.: Z. Phys. C – Particles and Fields 1 (1979) 343
42. CLEO Collab. D. Besson et al.: Phys. Rev. D 30 (1984) 1433
43. CLEO Collab. R. Giles et al.: Phys. Rev. Lett. 50 (1983) 877
44. CLEO Collab. P. Haas et al.: Phys. Rev. D 30 (1984) 1996
45. ARGUS Collab. H. Albrecht et al.: Z. Phys. C – Particles and Fields 28 (1985) 45
46. CLEO Collab. D. Andrews et al.: Phys. Rev. Lett. 50 (1983) 807
47. CUSB Collab. T. Kaarsberg et al.: Contributed paper to the 1987 International Symposium on Lepton and Photon Interactions at High Energies, Hamburg (1987)
48. PLUTO Collab. Ch. Berger et al.: Phys. Lett. 93 B (1980) 497
49. ARGUS Collab. H. Albrecht et al.: Z. Phys. C – Particles and Fields 35 (1987) 283